Eur. Phys. J. B **2**, 399–407 (1998)

THE EUROPEAN PHYSICAL JOURNAL B

Travelling pulses in reaction–diffusion systems under global constraints

H. Hempel[1,a], I. Schebesch[2], and L. Schimansky-Geier[1]

[1] Institut für Physik, Humboldt–Universität zu Berlin, Invalidenstraße 110, 10115 Berlin Germany
[2] Institut für Theoretische Physik, Technische Universität, Hardenbergstraße 36, 10623 Berlin, Germany

Received: 25 September 1997 / Revised: 9 January 1998 / Accepted: 9 January 1998

Abstract. The influence of global inhibition on travelling pulses both in infinite and in finite periodic systems is investigated. Analytic investigation of the modified piecewise linear Rinzel–Keller–Model (RKM) shows a shrinking and slowing down of pulses due to global inhibition. Analytic results obtained are confirmed by numerical simulations. The investigation is completed by numerical simulations of the modified Oregonator model for the light–sensitive BZR.

PACS. 52.35.Mw Nonlinear waves and nonlinear wave propagation (including parametric effects, mode coupling, ponderomotive effects, etc.)

1 Introduction

Reaction-Diffusion-Systems (RDS) have been used extensively to study structure formation in various physical systems. Excitable media are of most interest for the modelling of chemical nonlinear reactions, of the evolution of bacterial colonies and also of the behaviour of nonlinear semiconductors and gas-discharge processes [1–5]. They are described by a set of two reaction–diffusion equations with two effective components $u(x,t)$– the activator, $v(x,t)$– the inhibitor

$$\tau_u \frac{\partial}{\partial t} u = f(u,v) + {L_u}^2 \nabla^2 u \tag{1}$$

$$\tau_v \frac{\partial}{\partial t} v = g(u,v) + {L_v}^2 \nabla^2 v. \tag{2}$$

The usual shape of the nonlinear production and decay terms in these balance equations are an S-shaped activator- and a linear inhibitor–dynamics with one stable fixed point and a second long living branch that is responsible for the excited regime of the system [6–9]. The dynamics and hence the resulting structures in the medium are determined by the relation of the diffusion lengths L_u, L_v and relaxation times τ_u, τ_v. For $L_v \ll L_u$ and $\tau_u \ll \tau_v$, pulses travel with constant width L_0 and velocity c_0 through the medium if special boundary and initial conditions are applied.

The introduction of nonlocal couplings into these models is an important extension [10–13]. In this case the nonlinear production and decay in $f(u,v)$ and $g(u,v)$ do not only depend on the local value of the densities, but also on averages over a larger part or the entire system. In systems with one species, for instance, only nonlocal couplings were introduced to describe the ballast resistor [14,15]. Turing instabilities were also shown to be the result of a long–ranging nonlocal coupling [16].

Nonlocal couplings become global ones if their characteristic length is larger than the system size or the size of single structures. Their strength does not depend on the position anymore. The existence of such couplings is a very common feature of many physical systems. In catalytic surface reactions they occur in a natural way [17,18] because the adsorption processes depend on the local partial pressure which adjusts to the reaction on the surface. Global couplings are always present in nonlinear semiconductor devices where the overall current feeds back to the voltage applied [19,20]. They have been extensively investigated in electrochemical reactions [21]. In this paper we introduce a new way to control the light dependent Belousov–Zhabotinsky Reaction (BZR) globally. This reaction can be amplified or inhibited by controlling the intensity of light by the actual pattern formed in the reactor [22].

In the mathematical description a new time dependent parameter enters which must be determined self-consistently from the occurring structure. In the steady state it is a constant which shifts the characteristic parameters [23]. That is why these solutions belong to the same class of solutions as those without global coupling. However, global inhibition will change bifurcation points and, hence the conditions for the occurrence of the structure [13,24–28]. It yields complex interactions between several elementary structures [12,17,25,29,30].

[a] e-mail: harald@summa.physik.hu-berlin.de

In this paper we explore the influence of global inhibition on the most common structure in one dimensional excitable media which is the travelling pulse. A pulse exhibits an excitation of the media travelling with constant velocity. In excitable media with $L_v = 0$ both a stable and an unstable pulse are known to exist [6,31]. The influence of nonlocal coupling on the dynamics of pulses has already been discussed in [26]. Krischer and Mikhailov [25] have investigated the effect of global inhibition on the bifurcation from a standing to a travelling pulse.

We are interested in the dependence of the width L and the velocity c of a pulse on the coupling strength μ. We derive analytic relations for the shape and the velocity generalizing the solutions of Ito and Ohta [32] for the piecewise linear Rinzel–Keller model. The investigation is completed by numerical simulations of the modified Oregonator which describes the light-dependent BZR.

The special shape of the coupling differs in the two models. In the piecewise-linear model the threshold a is increased with the total sum of activator and inhibitor. We show in the next section that this situation can also be obtained from other kinds of couplings. In the Oregonator the incident light ϕ will be controlled by the total amount of activator. Despite the differences in both models the global coupling suppresses the excitability of the medium proportional to the amount of excited area in the medium. Therefore, it is not surprising that the results of both models coincide qualitatively and that our analytical approach can help to understand the findings for the Oregonator.

2 Analytical investigation of the globally inhibited RKM

2.1 The system

To study the influence of global inhibition on the velocity c and on the width L of a travelling pulse we considered a model with piecewise linear activator–inhibitor dynamics. Such models were first introduced by Rinzel and Keller [33] in 1973 and are analytically easily to treat [8,34,35,32].

$$\frac{\partial}{\partial t}u = -u - v + H(u-a) + \nabla^2 u \tag{3}$$

$$\epsilon^{-1}\frac{\partial}{\partial t}v = \gamma u - v. \tag{4}$$

Here the small factor ϵ is the ratio between the characteristic times of activator and inhibitor τ_u/τ_v, $H(u-a)$ is the Heavyside–function which is one if the activator exceeds the threshold value a. By the choice of the threshold $1/(1+\gamma) < a < a_{\mathrm{crit}} < 1/2$ we achieve excitability. The lower limit is characterized by the transition into the bistable regime and the upper limit $a = 1/2$ is the Maxwell point for the potential in equation (3) with $v = 0$. Moreover, we set $L_v = 0$ and $L_u = 1$. This model is known to exhibit a solitary travelling pulse for an overcritical initial condition, periodic boundary conditions – $u(0,t) = u(L_{\mathrm{Syst}},t), v(0,t) = v(L_{\mathrm{Syst}},t)$ or densities at infinity in the stable fixed point if $L_{\mathrm{Syst}} \to \infty$ [6,9].

The pulse is often discussed in terms of a front and a back interface within which v varies only slightly. In this approach the value of v within the interface determines its velocity. For the stationary pulse the value of v in the back interface will adjust such that its velocity becomes that of the front interface. If the distance of the interfaces is small an interaction has to be taken into account. Near the critical threshold a_{crit} the back interface acts on the front interface and the pulse will slow down. For overcritical $a > a_{\mathrm{crit}}$ the front interface stops whereas the back interface keeps on running until both interfaces collide and the pulse extincts. If ϵ is very small the back interface follows lately. Now the interaction between the interfaces is small and a_{crit} approaches $1/2$ where no positive interface velocity is possible anymore.

We introduced the global inhibition similar as in [25]

$$a = a_0 + \mu \int \mathrm{d}x' \left(u(x',t) + v(x',t)\right), \tag{5}$$

which results in a shift of the excitation value without changing the fixpoint value. μ stands for the coupling strength. The integral is taken over the whole system with length L_{Syst}. Both values are our new control parameters.

Another generic possibility to introduce global coupling in the activator dynamics is to modify equation (3) in the following way

$$\frac{\partial}{\partial t}u = -u - v + H(u-a_0) - \mu \int \mathrm{d}x' \left(u(x',t) + v(x',t)\right) + \nabla^2 u\,. \tag{6}$$

Here the global inhibition enters in an additive way and the threshold value a_0 is fixed. In this model the fixpoint $(u_{\mathrm{f}}, v_{\mathrm{f}})$ varies in dependence on the global amount of substrates on the system. This situation is more common in many experimental systems. As shown in Appendix A both kinds of inhibition are equivalent for stationary pulses. Equation (6) also yields a shift of an effective excitation threshold $\tilde{a}$ due to an effective coupling $\mu_{\mathrm{eff}} \propto \frac{\mu}{1+\mu L_{\mathrm{Syst}}}$. Note that μ_{eff} depends upon the system size and vanishes for large systems $L_{\mathrm{Syst}} \to \infty$.

In the analytic consideration we restrict ourselves to equations (3–5).

2.2 Stationary solutions

We are looking for travelling solutions of these equations (3–5) with a stationary shape, *i.e.*, $u(x,t) = u(z)$ and $v(x,t) = v(z)$ where $z = x - ct$. We define the length L of a pulse as the size of the area where $u(x) > a$, *i.e.*, $L = \int \mathrm{d}x H(u(x) - a)$. It is identical to the distance of the points where $\frac{\partial^2}{\partial x^2}u(x)$ changes its sign. Therefore, this definition seems to be a natural one.

This approach yields a system of ordinary differential equations. In Appendix B we explore the pulse solution of

equations (3, 4) given in [32]. The new point in our investigation is that the excitation value a becomes a function of the shape of the travelling pulse.

As in [24] we use a self–consistent approach. For a stationary pulse the threshold a will be constant. We look for a family of solutions $u(x), v(x)$ of equations (3, 4) depending parametrically on a. Hence, the velocity and the width are functions of a. The knowledge of these functions gives the key to solve the full problem where a itself depends on integrals over the solution $u(x), v(x)$ due to equation (5). In this equation a should be determined self–consistently. If the integral in equation (5) could be evaluated straightforward we would obtain a single equation for a. We will see that in our case equations (3, 4) yield a closed set of two equations for c and L. They remain closed if we take equation (5) into account. These equations must be solved for special values of μ, ϵ, γ and a_0. Since we are not interested in a solution for special parameters we determine the inverse relation, *i.e.*, a_0 as a function of a. This is more convenient since equation (5) can immediately be solved for a_0. The relation obtained reveals the qualitative behaviour of the family of solutions for different parameters.

It remains to calculate the expression of the integral in equation (5). From equation (3) we find for a travelling pulse

$$\int \mathrm{d}x' \left(u(x') + v(x')\right) = \int \mathrm{d}x' H(u-a) = L. \tag{7}$$

We obtain an increase of the excitation value a with the width of the pulse L.

Using equation (4) we are able to calculate the contribution of the activator and inhibitor separately

$$\int \mathrm{d}x' u(x') = \frac{1}{\gamma} \int \mathrm{d}x' v(x'). \tag{8}$$

It becomes clear that every kind of global inhibition that is linear in u and v scales with the width L of the pulse and will, therefore, behave similarly to our model.

2.3 Single pulse for $L_{\mathrm{Syst}} \to \infty$

Let us first consider a single solitary pulse (Fig. 1) in an infinite extended media of equations (3–5) with densities at the boundaries $(u, v)\,|_{z\to\pm\infty} = (u_\mathrm{f}, v_\mathrm{f}) = (0, 0)$. It requires the solution of several merging conditions and

$$u(0) = u(L) = a. \tag{9}$$

We use the solution of Ito and Ohta parametrically dependent on a given in Appendix B. Taking into account the global inhibition it leads to the following set of transcendental equations:

$$\frac{h(\lambda_1)}{\lambda_1 P'(\lambda_1)} \left(1 - \mathrm{e}^{\lambda_1 L}\right) = a_0 + \mu L, \tag{10}$$

$$\sum_{i=2}^{3} \frac{h(\lambda_i)}{\lambda_i P'(\lambda_i)} \left(1 - \mathrm{e}^{-\lambda_i L}\right) = a_0 + \mu L\,. \tag{11}$$

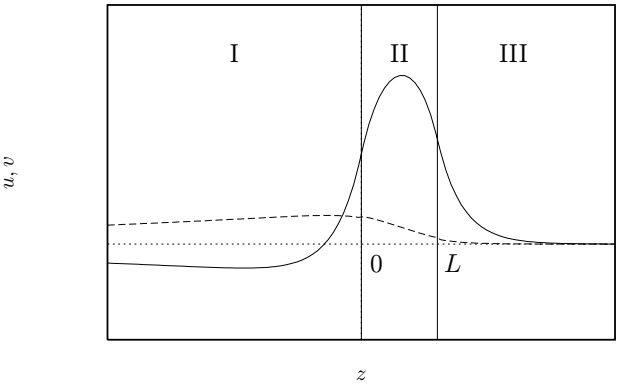

Fig. 1. Shape of a pulse. The solid line corresponds to the activator concentration $u(z)$ and the dashed line to the inhibitor concentration $v(z)$. There are three sections – the front section III, the excited section II and the back section I.

As shown in Appendix B the eigenvalues λ_i and also functions P, h and k are parametrically dependent on c. Therefore equations (10, 11) completely determine the aimed velocity c and L.

To obtain analytical expressions we assume $\epsilon \ll 1$ and $c \propto \epsilon^{1/2}$. In this case the length L of the pulse is comparable to the diffusion length of the activator $L \propto \mathcal{O}(1)$, *i.e.* the width of the interfaces and the entire pulse are of the same order. Equations (10, 11) give in $\mathcal{O}(\epsilon^{1/2})$

$$c^2 = \epsilon\gamma \left(-3 + \frac{2}{\frac{1}{L} - \frac{1}{\mathrm{e}^L - 1}} \right) \tag{12}$$

$$a_0 + \mu L = \frac{1 - \mathrm{e}^{-L}}{2} - \frac{\epsilon\gamma L}{2c}. \tag{13}$$

The strength of global inhibition contributes only in equation (13) with the magnitude of order $\mathcal{O}(1)$. This new term changes the behaviour of the stable branch of the solution where $\mathrm{d}L/\mathrm{d}a_0 < 0$. In the case $\mu = 0$ only the term $\epsilon\gamma L/(2c)$ gives rise to a stable branch, and a_0 lies in the vicinity of the Maxwell point $1/2$ [35]. For a_0 considerable smaller than $1/2$ our *ansatz* $c \propto \epsilon^{1/2}$ fails. In contrast, if $\mu = \mathcal{O}(1)$ the given approximation yields an upper branch for arbitrary a_0 below the critical one. Now the term due to global interaction in equation (13) dominates the adjustment of the width of the pulse. We can neglect the term proportional to ϵ in equation (13) and this equation will determine L. In this equation γ no longer appears. However, it cannot be chosen arbitrarily since only in excitable media where $\gamma > 1/a - 1$ travelling pulses exist.

Equation (12) gives a monotonous relation between c and L. This relation is depicted in Figure 2. Larger pulses possess higher velocities. This curve does not distinguish between stable and unstable solutions. We underline that the relation does not depend on μ. However, the stability of the pulse will depend strictly on μ.

The graph $L(\mu)$ is shown in Figure 3. It was obtained by plotting the inverse function $\mu(L)$ from equation (13). For a fixed μ below some critical value a stable large and an unstable small inhomogeneous solution exist. We also

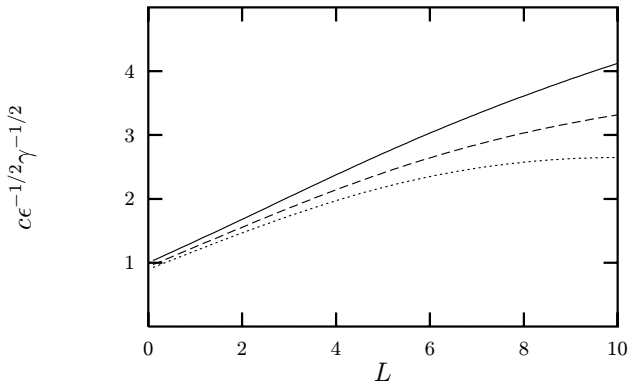

Fig. 2. Dependence of velocity c on the size of the pulse L, solid line in an infinite system, dashed line $L_{\rm Syst} = 33.3$, dotted line $L_{\rm Syst} = 20.0$.

show the dependence of c on μ (Fig. 3). Both values in the stable branch are monotonously decreasing as μ increases. The amplitude $u_{\max}$ of the pulse up to $\mathcal{O}(\epsilon^{1/2})$ given by

$$u_{\max} = 1 - \mathrm{e}^{-L/2} - \frac{\epsilon\gamma L}{2c} \tag{14}$$

decreases for increasing μ (Fig. 3).

In the limit $\mu \gg \sqrt{\epsilon\gamma}\,\mathcal{O}(1)$ the saddle–node bifurcation of the two inhomogeneous solutions can be estimated analytically. At the bifurcation point the width L approaches the value

$$L^{(\mathrm{SNB})} = -\log 2\mu, \tag{15}$$

which inserted in equation (13) gives the bifurcation threshold

$$a_0^{(\mathrm{SNB})} = \frac{1}{2} - \mu - \mu\log 2\mu. \tag{16}$$

This dependence is depicted in Figure 4. Above $a_0^{(\mathrm{SNB})}$ no inhomogeneous solitary pulse solution exists. In Figure 3 the dotted lines show the bifurcation values. These values are in good agreement with the turning points of the curves obtained for small ϵ. We underline that the bifurcation values of c, L and $u_{\max}$ decrease with increasing coupling strength μ. Hence, smaller stable pulses can be realized by increasing global inhibition.

2.4 Pulses on a ring

Now we discuss travelling pulses on a ring. Since periodic boundary conditions are applied equations (10, 11) modify to

$$\sum_{i=1}^{3} \frac{h(\lambda_i)\left(1-\mathrm{e}^{\lambda_i L}\right)}{\lambda_i P'(\lambda_i)\left(1-\mathrm{e}^{\lambda_i L_{\rm Syst}}\right)} = a_0 + \mu L, \tag{17}$$

$$\sum_{i=1}^{3} \frac{h(\lambda_i)\left(1-\mathrm{e}^{-\lambda_i L}\right)}{\lambda_i P'(\lambda_i)\left(1-\mathrm{e}^{-\lambda_i L_{\rm Syst}}\right)} = a_0 + \mu L, \tag{18}$$

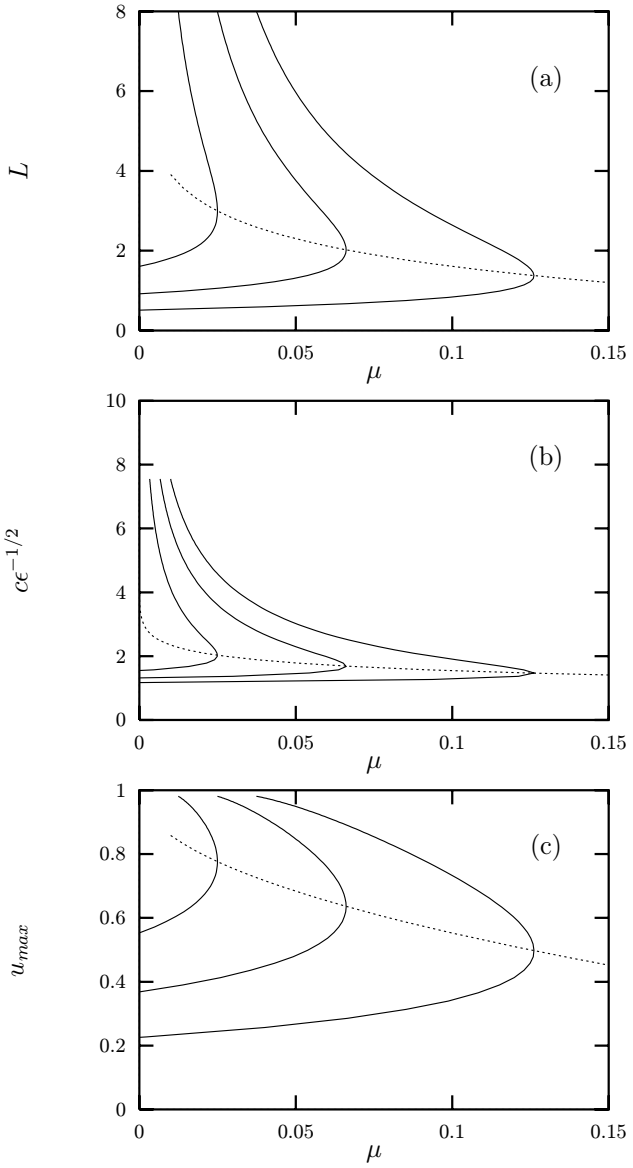

Fig. 3. Dependence of the order parameter on μ for $a_0 = 0.2, 0.3, 0.4$ for the piecewise linear model where $L_{\rm Syst} \to \infty$ (width L (a), velocity c (b) and amplitude $u_{\max}$ (c)). Dotted lines represent values at the saddle-node-bifurcation. All values are exact up to $\mathcal{O}(\epsilon^{1/2})$.

where the system size $L_{\rm Syst}$ enters. The polynomials P, h and the eigenvalues are the same as in equations (10, 11). Equations (10, 11) are obtained for $L_{\rm Syst} \to \infty$.

Equations (17, 18) yield up to $\mathcal{O}(1)$

$$a_0 + \mu L = \frac{\sinh\left(\frac{L}{2}\right)\cosh\left(\frac{L_{\rm Syst}-L}{2}\right)}{\sinh\left(\frac{L_{\rm Syst}}{2}\right)} - \frac{L\gamma}{L_{\rm Syst}(1+\gamma)}. \tag{19}$$

We find another term $\frac{L\gamma}{L_{\rm Syst}(1+\gamma)}$ due to finite size which leads to a shrinking of pulses. It acts similarly to global inhibition. In fact, it is the main difference to equation (13). The reason for the existence of this term can be explained easily. The pulse permanently travels through

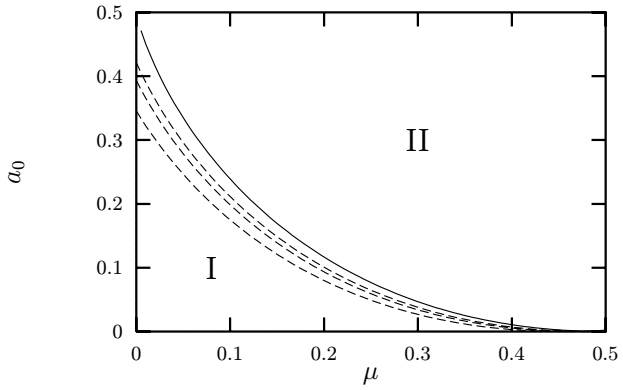

Fig. 4. Bifurcation-line for $L_{\mathrm{Syst}} \to \infty$ – solid line and $L_{\mathrm{Syst}} = 20, 33, 50$ – dashed lines. Pulses exist below the lines in region I. In region II no pulses solution exist. The larger L_{Syst} the larger region I.

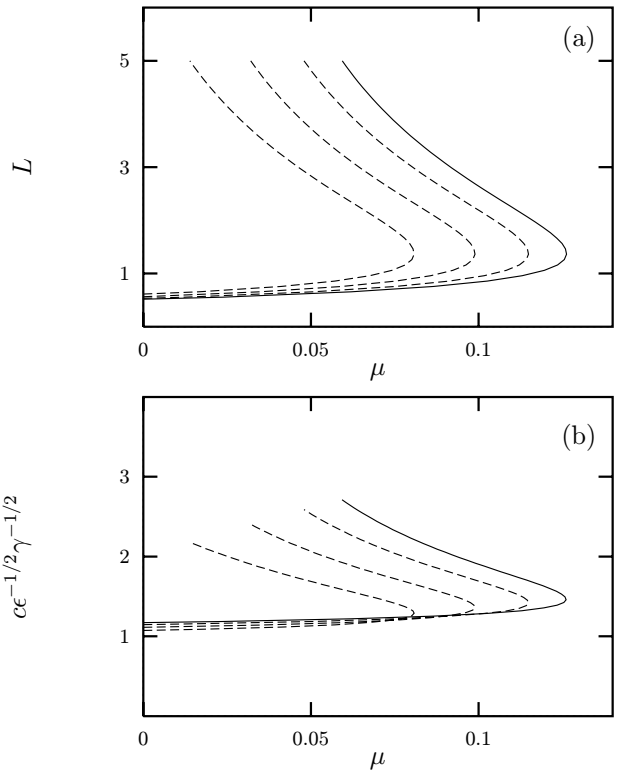

Fig. 5. Width L (a) and velocity c (b) of a pulse in dependence on the system size – solid infinite system, dashed line $L_{\mathrm{Syst}} = 80$, $L_{\mathrm{Syst}} = 33.3$, $L_{\mathrm{Syst}} = 20$.

the medium producing inhibitor. The decay time of the inhibitor is large in comparison to the time of a walk of the pulse around the ring. Therefore a homogeneous stationary background of the inhibitor is always present in the system leading to an effective shift of the threshold. Other modifications between equations (13, 19) are of importance if L_{Syst} becomes rather small. The width of a pulse in a finite periodic system is shown in Figure 5a.

Further expansion of equations (17, 18) up to $\mathcal{O}(\epsilon^{1/2})$ yields a relation between velocity and width of the pulse given in Appendix B. It is depicted in Figure 2. The pulses become slower and smaller as the system size L_{Syst} decreases (Fig. 5). This is the typical behaviour for wave trains in dependence on the wavelength. We reestablish this fact here for globally inhibited finite systems. The dependence on the period T is also similar to that of wave trains (Fig. 6). The minimal period $T_{\min}$ increases in a globally inhibited system.

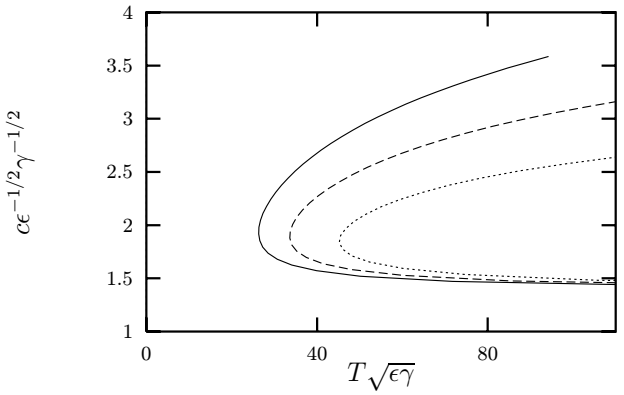

Fig. 6. Dependence of the velocity of a pulse in a ring on the period T for $\mu = 0$ – solid line, $\mu = 0.02$ – dashed line and $\mu = 0.04$ – dotted line.

The position of the saddle–node bifurcation is given by

$$a_0^{(\mathrm{SNB})} = -\mu L^{(\mathrm{SNB})} + \frac{\sinh\left(\frac{L^{(\mathrm{SNB})}}{2}\right)\cosh\left(\frac{L_{\mathrm{Syst}}-L^{(\mathrm{SNB})}}{2}\right)}{\sinh\left(\frac{L_{\mathrm{Syst}}}{2}\right)} - \frac{L^{(\mathrm{SNB})}\gamma}{L_{\mathrm{Syst}}(1+\gamma)} \tag{20}$$

with the width L at the bifurcation point

$$L^{(\mathrm{SNB})} = \frac{L_{\mathrm{Syst}}}{2} - \operatorname{arccosh}\left\{2\sinh\left(\frac{L_{\mathrm{Syst}}}{2}\right)\left(\mu + \frac{\gamma}{L_{\mathrm{Syst}}(1+\gamma)}\right)\right\}. \tag{21}$$

It is depicted in Figure 4. The parameter region where stable pulses can be observed shrinks as the system size L_{Syst} decreases.

It is obvious how to construct more complicated solutions which consist of several pulses using the described solution subject to periodic boundary conditions. In this case a solution of two pulses on a ring is constructed out of the single pulse solution in the system with size $L_{\mathrm{Syst}}/2$. The solutions obtained in this way are parts of a wave train. A bifurcation diagram of these solutions is depicted in Figure 7.

2.5 Numerical investigation

We carried out simulations of the RKM for $L_{\mathrm{Syst}} = 20$ using an explicit Euler–method on a lattice of 1000 grid-points with periodic boundaries. For reasons of numerical convenience we chose a tanh–function with a certain width

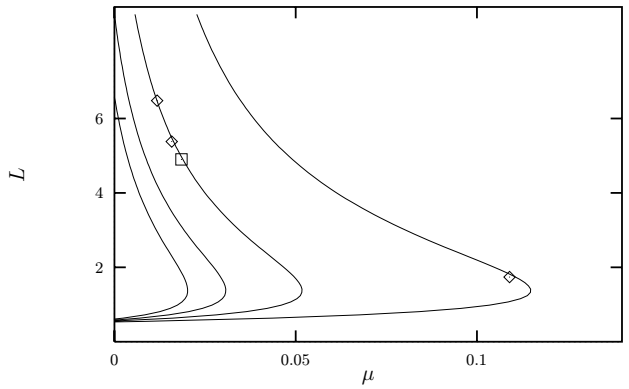

Fig. 7. Size of one, two, three and four pulses for $L_{\mathrm{Syst}} = 80$ (right to left). Parameters: $a_0 = 0.2$, $\gamma = 10$, $\epsilon \to 0$. Numerically ($\epsilon = 5 \times 10^{-4}$) we found stable pulses at ($\diamond$). At ($\square$) two pulses are unstable, one decays and the other survives jumping to the branch of a single pulse.

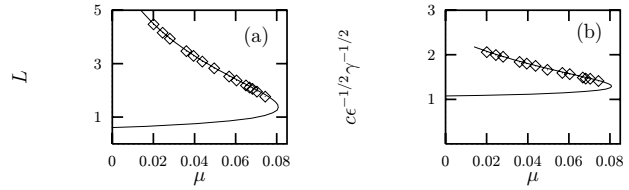

Fig. 8. Numerically obtained size (a) and velocity (b) of pulses in the RKM for $L_{\mathrm{Syst}} = 20$, $\gamma = 10$, $\epsilon = 5 \times 10^{-4}$ ($\diamond$), solid line – value obtained by analytical calculation for $\epsilon \to 0$. Since we use a finite ϵ in our simulations deviations from the analytic results occur.

instead of $H(x)$ as nonlinearity. In order to investigate the stability of the solution, we added small noise in the simulation. The results of these simulations are in good agreement with those obtained analytically for $\epsilon \to 0$. Small deviations from the exact analytic expressions are due to the modification of the nonlinearity in our system, and the finite ϵ we had to introduce. Moreover, they prove the stability of the large pulses, *i.e.*, the upper branch in Figure 8. Single pulses on the lower branch in Figure 8 are unstable in our simulation.

Additionally, we investigated the behaviour of two pulses on a ring. This solution is composed of two single pulses on rings of half the system size and half value of global coupling. The simulation reveal that two pulses are not stable at the entire upper branch. We found stable two pulses for rings larger than $L_{\mathrm{Syst}} = 80$ (Fig. 7) and μ smaller than a critical one. For large μ it happened that one pulse was growing and the other shrinking. This instability of two pulses is due to their interaction both *via* global inhibition and the action of the inhibitor v. A perturbation which enlarges one pulse will increase the threshold a. Furthermore the pulse produces more inhibitor v locally which affects the pulse coming next, i.e, the smaller one. Obviously, both kinds of interaction make the motion of the second pulse more unfavourable and, thus, the second pulse shrinks. Therefore, two pulses are only stable for large rings and for small global coupling μ.

3 Influence of light-induced global feedback in the Oregonator-model

Now we start to investigate the effect of a global coupling on a well suited experimental system for the study of travelling waves [36–39]. We consider the light sensitive Belousov-Zhabotinskii reaction with rutheniumbipyridyl as a catalyst. Global feedback–effects were realized in this system [40]. Another global coupling can be introduced by measuring the transmitted light intensity through a Petri dish and feeding it back to the incident light. The theoretical modelling of this situation will be the subject of this section.

The modified Oregonator model can be regarded as a first approximation to describe the dynamics of this reaction on a qualitative level and reads

$$\frac{\partial}{\partial t}u = \frac{1}{\epsilon}\left[u(1-u) - (\gamma v + \phi)\frac{u-q}{u+q}\right] + D_u\nabla^2 u \quad (22)$$

$$\frac{\partial}{\partial t}v = u - v + D_v\nabla^2 v. \quad (23)$$

Here u and v again play the role of activator and inhibitor, respectively. u denotes the local concentration of $HBrO_2$ and v the oxidized form of the catalyst scaled by the rate constants of the five reaction steps the Oregonator takes into account and by the recipe to bring the parameters into dimensionless quantities [31]. The relation of the time scales ϵ as well as q are determined by rate constants and the chemical concentrations. γ is a stoichiometric parameter that appears in that reaction of the Oregonator scheme which describes the release of bromide ions by the oxidation of bromalonic and malonic acid. D_u and D_v are the diffusion coefficients of the two species. ϕ is the photochemically produced bromide flow which describes the influence of the incident light. Both γ and ϕ determine the excitation threshold of the system.

Our global feedback will be realized by variation of the incident light. The spatial average of the emerging pattern determines the forthcoming evolution *via* the incident light [22]. This light-induced global feedback is introduced into the system *via* a third equation. It describes the temporal changes in the photochemically produced bromide flow

$$\phi = \phi_0 + \mu \int u(x',t)\,\mathrm{d}x'. \quad (24)$$

This dynamics, therefore, gives the global feedback by the integral over the activator which now not necessarily scales with the width of the pulse.

Nevertheless, the type of this global coupling is similar to the situation considered in previous sections. The variation of the incident light leads to a shift of the activator nullcline $\dot{u} = 0$. However, this nullcline is very steep in the vicinity of the fixpoint. So the activator concentration in the fixpoint changes only slightly and therefore the contribution of the fixpoint to the integral becomes negligible. In fact, inclusion of the global feedback results in a shift of the excitation value proportional to the total amount

of activator. Hence, it is not surprising that we will obtain similar results as in the previous section.

In order to study the influence of the strength of the global feedback on the dynamics of solitary pulses numerical simulations of equations (22–24) are carried out in the excitable regime. These simulations are performed using a finite-difference scheme with up to 8000 equidistant gridpoints and periodic boundary conditions. The set of the ODEs is solved using an explicit Euler-method. A solitary pulse is used as initial distribution. For the simulations presented in this paper the values of q, ϵ, γ ,ϕ_0 , D_u and D_v are fixed at $q = 0.002$, $\epsilon = 0.01$, $D_u = 1.0$, $D_v = 0.6$, $\gamma = 3.0$, $\phi_0 = 0.01$.

A set of simulations shows that the pulse profile, the pulse amplitude and the propagation speed can be controlled by the global feedback (Fig. 9). Increasing the strength of the global interaction μ leads to a decay of the propagation speed and the width of the pulse. At the same time the amplitude of the pulse decreases. However, the propagation speed cannot drop to zero. In fact, the pulse will disappear with finite width, amplitude and velocity when a critical value of the coupling strength is reached. This behaviour is in good agreement with the analytical results obtained in the previous section (see Fig. 3). The relation between size and velocity of a pulse obtained numerically is shown in Figure 10. The data do not reveal any dependence on the system size. Basically, there is the same dependence as that found for the RKM (Fig. 2). It becomes detectable if $L/L_{\rm Syst}$ becomes larger. However, simulations in this regime of pulse widths are very time consuming since they require the choice of a very small ratio of time scales ϵ.

Furthermore, we investigated the stability of two pulses. Here again an instability was found in regions where the corresponding single pulse solution is stable. For large systems $L_{\rm s} > 200$ two pulses can coexist. They become unstable for a critical μ about 9.

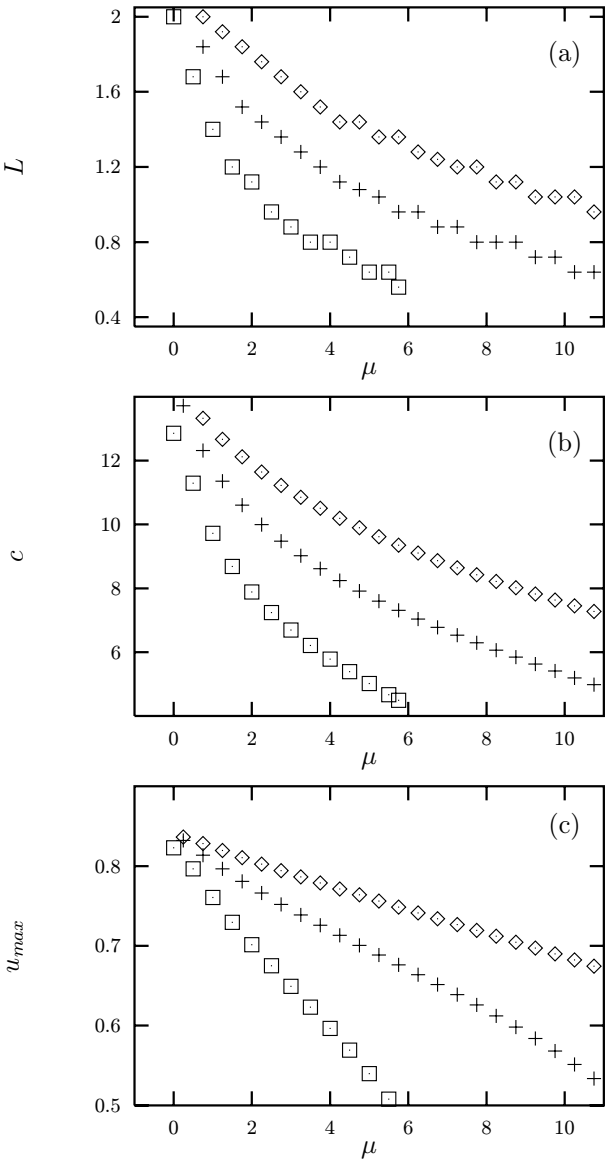

Fig. 9. Width (a), velocity (b) and amplitude (c) of a solitary pulse versus the coupling strength at fixed parameters γ and ϕ_0. The width of the pulse was determined at $u = u_{\rm max}/2$, ($\diamond$) for $L_{\rm Syst} = 200$, (+) for $L_{\rm Syst} = 80$, ($\Box$) for $L_{\rm Syst} = 30$.

4 Conclusion

We considered theoretic models where a global coupling feeds back *via* a inhibitory shift of the excitation threshold. This situation seems to be a general one since an additive kind of global inhibition can be transformed into our model. Global inhibition results in the shrinking of pulses of excitation over several orders of magnitude. The velocity of the pulses decreases strongly if global inhibition is switched on.

We have studied the propagation of a globally inhibited solitary pulse in an infinite medium and in ring–like devices. We have shown that finite system lengths lower the width and the velocity of a pulse. The parameter region for stable pulses shrinks with the system size. These two phenomena are well known for media without global inhibition. In this work we have investigated them quantitatively. We have found exact analytic expressions for both the shape and the velocity of the pulse. It was proven numerically that the upper branch of the single pulse solution is stable and the lower branch is unstable. Global coupling stabilizes smaller pulses. We emphasize that our results obtained in finite systems using periodic boundary conditions can also be applied to wave trains. Numerical simulations of two pulses revealed that they are not stable on the entire upper branch but stable above some critical width.

If the ratio of the time scales of activator and inhibitor is arbitrary small the shape of the pulse in an infinite system is governed by the strength of global inhibition μ and not by the coupling of the local inhibitor γ. However, $\gamma > 0$ is required in order to realize an active media. Therefore, the pulse is not sensitive to a small adiabatic fluctuation of the properties of the dynamics of the inhibitor v as long as an excitable media is realized.

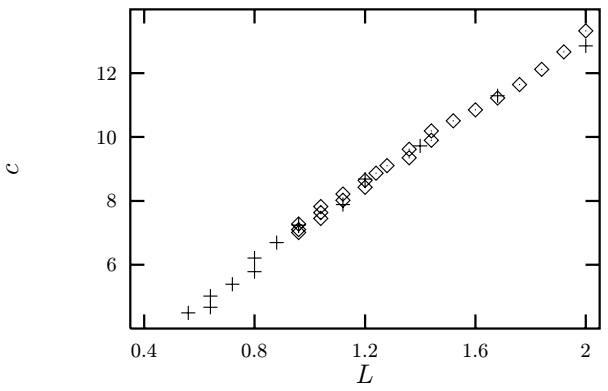

Fig. 10. Numerically obtained relation between size and velocity of a pulse when varying the incident light ϕ, ($\diamond$) for $L_{\mathrm{Syst}} = 200$, (+) for $L_{\mathrm{Syst}} = 30$.

Inclusion of global inhibition in the light sensitive BZR, which was realized *via* a control of the incident light, also gives rise to a shift of the excitation value. Therefore, numerical results for the Oregonator are in qualitative agreement with those for the RKM. The dependence on the system size found in the two models behaves similarly.

Global inhibition provides a mechanism for controlling and manipulating spatio–temporal behaviour of active media. It is a possible way to control the velocity of a pulse experimentally. Furthermore, one can restrain a pulse by applying strong global inhibition and let it go at will switching off global inhibition.

Since only one pulse is stable for overcritical global couplings wave train solutions can be suppressed. Hence, the behaviour of a global inhibited pulse generator will change too. It remains still a challenge to investigate this in greater detail. It seems feasible to build a pulse generator which takes the values of global coupling as input data and generates nonperiodic wave trains in a definite way. One can imagine that it can be used to prepare special initial conditions or even to generate messages.

We highly appreciate financial support from DFG–grant SCHI–354.

Appendix A: Additive global inhibition

We investigate the relation between the systems on the one hand equations (3–5) and on the other hand equations (4, 6). Applying a linear transformation in the system equations (4, 6) with additive inhibition

$$\tilde{u} = u - u_{\mathrm{f}} = u + \frac{\mu}{1+\gamma} \int \mathrm{d}x' \left(u(x',t) + v(x',t)\right) \quad (25)$$

$$\tilde{v} = v - v_{\mathrm{f}} = v + \frac{\gamma\mu}{1+\gamma} \int \mathrm{d}x' \left(u(x',t) + v(x',t)\right) \quad (26)$$

and a varying threshold value

$$\tilde{a} = a_0 + \frac{\mu}{(1+\gamma)(1+\mu L_{\mathrm{Syst}})} \int \mathrm{d}x' \left(\tilde{u}(x',t) + \tilde{v}(x',t)\right) \quad (27)$$

we find that the inhibitor dynamics equation (4) does not change and the activator dynamics equation (6) reads

$$\frac{\partial}{\partial t}\tilde{u} = -\tilde{u} - \tilde{v} + H(\tilde{u} - \tilde{a}) + \nabla^2 \tilde{u} - \frac{\mu}{1+\mu L_{\mathrm{Syst}}} \frac{\mathrm{d}}{\mathrm{d}t} \int \mathrm{d}x' \left(\tilde{u}(x',t) + \tilde{v}(x',t)\right). \quad (28)$$

We obtained a dynamics like in equations (3–5) with globally inhibited excitation value $\tilde{a}$ due to equation (27). An additional term describes the change of the total amount of substrates. However, for the travelling pulses this term vanishes. Moreover, the fixpoint $(u_{\mathrm{f}}, v_{\mathrm{f}})$ given by the integrals in equations (25, 26) becomes stationary. Therefore, both generic cases can be mapped one onto the other for travelling pulses.

However, in contrast to the first kind of global coupling the strength of the coupling depends on the system size L_{Syst}. An effective coupling $\mu_{\mathrm{eff}} \propto \frac{\mu}{1+\mu L_{\mathrm{Syst}}}$ occurs in equation (27) which saturates for large μ. For large systems $L_{\mathrm{Syst}} \to \infty$ the coupling μ_{eff} tends to zero. For single solitary pulses we assume (Eq. (7))

$$\int \mathrm{d}x' \left(\tilde{u}(x',t) + \tilde{v}(x',t)\right) = \tilde{I} = \mathrm{const} \ll L_{\mathrm{Syst}}.$$

Therefore, there is no change of the threshold value $\tilde{a} = a_0$ in equation (27) for infinite systems. The fixpoint value in this situation tends to the original value $(u_{\mathrm{f}} = 0, v_{\mathrm{f}} = 0)$. This becomes clear from the calculation of the integral

$$I = \int \mathrm{d}x' \left(u(x',t) + v(x',t)\right) = L_{\mathrm{Syst}}(u_{\mathrm{f}} + v_{\mathrm{f}}) + \int \mathrm{d}x' \left(\tilde{u}(x',t) + \tilde{v}(x',t)\right) = I_0 + \tilde{I}.$$

Using the expressions for the fixpoint equations (25, 26) we find vanishing solutions $u_{\mathrm{f}}, v_{\mathrm{f}}$ for $L_{\mathrm{Syst}} \to \infty$. Therefore, for $L_{\mathrm{Syst}} \to \infty$ there are no effects in infinite systems with additive inhibition of the type of equations (3, 4, 6). Only for $L_{\mathrm{Syst}} < 1/\mu$ strong effects result from the additive inhibition. The problems of equations (3, 4, 6) can be mapped to problems with shifting excitation threshold.

Appendix B: Pulse-solution in the Rinzel-Keller-model

According to [32] we obtain a solution of equations (3, 4) in several steps. First we divide the solution into three sections for z according to the values of u (see Fig. 1). Within section II and III we have $u(z) < a$, and in section II there is $u(z) > a$. Without loss of generality we set

the boundary between section I and II to $x_1 = 0$. The position of the boundary between II and II has yet to be determined. We denote it by $x_2 = L$. Here L can be interpreted as the length of excitation or the width of the pulse.

We have in each section

$$\begin{pmatrix} u(z) \\ v(z) \end{pmatrix} = \begin{pmatrix} \frac{1}{1+\gamma} \\ \frac{\gamma}{1+\gamma} \end{pmatrix} H(u-a) + \sum_{i=1}^{3} A_i^{(\text{section})} \begin{pmatrix} -h(\lambda_i) \\ \gamma \end{pmatrix} \mathrm{e}^{\lambda_i z}, \quad (29)$$

where

$$h(\lambda) = (c\lambda - \epsilon)/\epsilon.$$

λ_i are the zeros of

$$P(\lambda) = (\lambda^2 + c\lambda - 1(\lambda)h(\lambda) + \gamma = 0. \quad (30)$$

Assuming that $c > 0$ this yields three solutions $\lambda_1 < 0 < \lambda_2 < \lambda_3$.

In order to solve the full problem we have to determine the coefficients $A_i^{(\mathrm{I})}$ in each interval. This can be done by applying several fit and boundary conditions. We end up with two transcendental equations in L and c which are

$$u(0) = u(L) = a. \quad (31)$$

They yield equations (10, 11).

In a finite periodic system we have to consider only two sections where $u(z) > a$ and $u(z) < a$, respectively. So equation (29) still holds for two sections. Consequently, the matching conditions become

$$u(0) = u(L) = u(L_{\mathrm{Syst}}) = a, \quad (32)$$

which lead to equations (17, 18).

An expansion in orders of $\epsilon^{1/2}$ yields an expression of the velocity

$$c^2 = \epsilon\gamma \frac{N}{M} \quad (33)$$

where

$$\begin{aligned} N = {} & 4L(1 - \frac{L}{L_{\mathrm{Syst}}}) \sinh^2\left(\frac{L_{\mathrm{Syst}}}{2}\right) + (L_{\mathrm{Syst}} - L)\cosh L \\ & - L_{\mathrm{Syst}} + L\cosh(L_{\mathrm{Syst}} - L) \\ & - 12\sinh\left(\frac{L_{\mathrm{Syst}}}{2}\right)\sinh\left(\frac{L_{\mathrm{Syst}} - L}{2}\right)\sinh\left(\frac{L}{2}\right) \\ M = {} & 4\sinh\left(\frac{L_{\mathrm{Syst}}}{2}\right)\sinh\left(\frac{L_{\mathrm{Syst}} - L}{2}\right)\sinh\left(\frac{L}{2}\right) \\ & - (L_{\mathrm{Syst}} - L)\cosh L - L\cosh(L_{\mathrm{Syst}} - L) + L_{\mathrm{Syst}}. \end{aligned}$$

References

1. E. Schöll, *Nonequilibrium Phase Transitions in Semiconductors* (Springer, Berlin etc., 1987).
2. M.C. Cross, P.C. Hohenberg, Rev. Mod. Phys. **65**, 851 (1993).
3. A. Brandl, W. Prettl, Phys. Rev. Lett. **66**, 3044 (1991).
4. K. Krischer, M. Eiswirth, G. Ertl, J. Chem. Phys. **96** (1992), 9161.
5. J.D. Murray, *Mathematical biology* (Springer, Berlin, 1989).
6. J.J. Tyson, J.P. Keener, Physica D **32**, 327 (1988).
7. Y.A. Vasilev, Yu.M. Romanovsky, D.S. Chernavsky, V.G. Yakhno, *Autowave processes in kinetic systems* (Deutscher Verlag der Wissenschaften, Berlin, 1989).
8. A.S. Mikhailov, *Foundation of synergetics* (Springer, Berlin, 1990).
9. B.S. Kerner, W.W. Osipov, *Autosolitons* (Kluwer, Dordrecht, 1994).
10. L. Schimansky-Geier, C. Zülicke, E. Schöll, Z. Phys. B **84**, 433 (1991).
11. V. Hakim, W.J. Rappel, Phys. Rev. A **46**, 7347 (1992).
12. B. Meerson, P.V. Sasorov, Phys. Rev. E **53**, 3491 (1996).
13. L.M. Pismen, J. Chem. Phys. **101**, 3135 (1994).
14. R. Landauer, Phys. Rev. A **15**, 2117 (1977).
15. D. Bedeaux, P. Mazur, Physica A **105**, 1 (1981).
16. B.N. Belintsev, M.A. Lifshitz, M.V. Volkenstein, Phys. Lett. A, **82**, 20 (1981).
17. F. Mertens, R. Imbihl, A. Mikhailov, J. Chem. Phys. **101**, 9903 (1994).
18. M. Bär, M. Hildebrand, M. Eiswirth, M. Falcke, H. Engel, M. Neufeld, Chaos Solit. Fract. **4**, 499 (1994).
19. F.J. Niedernostheide, B.S. Kerner, H.G. Purwins, Phys. Rev. B **46**, 7559 (1992).
20. A. Wacker, E. Schöll, Z. Phys. B **93**, 431 (1994).
21. U. Middya, M.D. Graham, D. Luss, M. Sheintuch, J. Chem. Phys. **98**, 2823 (1993).
22. I. Schebesch, H. Engel, *Influence of a light–induced global coupling on the dynamics of waves in the BZR*, edited by H. Engel, E. Schöll, F.J. Niedernostheide (Verlag Wissenschaft & Technik, 1996).
23. R. Bartussek, C. Zülicke, L. Schimansky-Geier, Chaos Solit. Fract. **5**, 1927 (1995).
24. L. Schimansky-Geier, H. Hempel, R. Bartussek, and C. Zülicke, Z. Phys. B **96**, 417 (1995).
25. K. Krischer, A. Mikhailov, Phys. Rev. Lett. **73**, 23 (1994).
26. M.D. Graham, U. Middya, D. Luss, Phys. Rev. E **48**, 2917 (1993).
27. R. Woesler, P. Schütz, M. Bode, M. Or-Guil, H.G. Purwins, Physica D **91**, 376 (1996).
28. M. Suzuki, T. Ohta, M. Mimura, H. Sakaguchi, Phys. Rev. E **52**, 3645 (1995).
29. S. Ei, T. Ohta, Phys. Rev. E **50**, 4672 (1994).
30. H. Hempel, L. Schimansky-Geier, *Localized structures in a two-dimensional system*, edited by H. Engel, E. Schöll, F.J. Niedernostheide (Verlag Wissenschaft & Technik, 1996).
31. J.J. Tyson, J.P. Keener, Physica D **21**, 307 (1986).
32. A. Ito, T. Ohta, Phys. Rev. A **45**, 8374 (1992).
33. J. Rinzel, J.B. Keller, Biophys. J. **13**, 1313 (1973).
34. S. Koga, Y. Kuramoto, Prog. Theor. Phys. **63**, 106 (1980).
35. A.S. Mikhailov, V.I. Krinsky, Physica D **9**, 346 (1983).
36. S.C. Müller, T. Plesser, B. Hess, Physica D **24**, 71 (1987).
37. M. Braune, A. Schrader, H. Engel, Chem. Phys. Lett. **222**, 358 (1994).
38. M. Braune, H. Engel, Chem. Phys. Lett. **204**, 257 (1993).
39. O. Steinbock, S.C. Müller, Phys. Rev. E **47**, 1506 (1993).
40. S. Grill, V.S. Zykov, S. C. Müller, Phys. Rev. Lett. **75**, 3368 (1995).